Discover Applied Sciences

Research

Applying UPLC-QTOF-MS/MS to profile the phytochemical constituents associated with docking studies of major components of *Ziziphora capitata* L as well as antimicrobial and antioxidant activity assessments of its subsequent fractions

Youssif M. Youssif[1] · Ahmed Ragab[2] · Medhat A. Zahran[2] · Fatma A. Ahmed[1] · Gameel A. M. Elhagali[2]

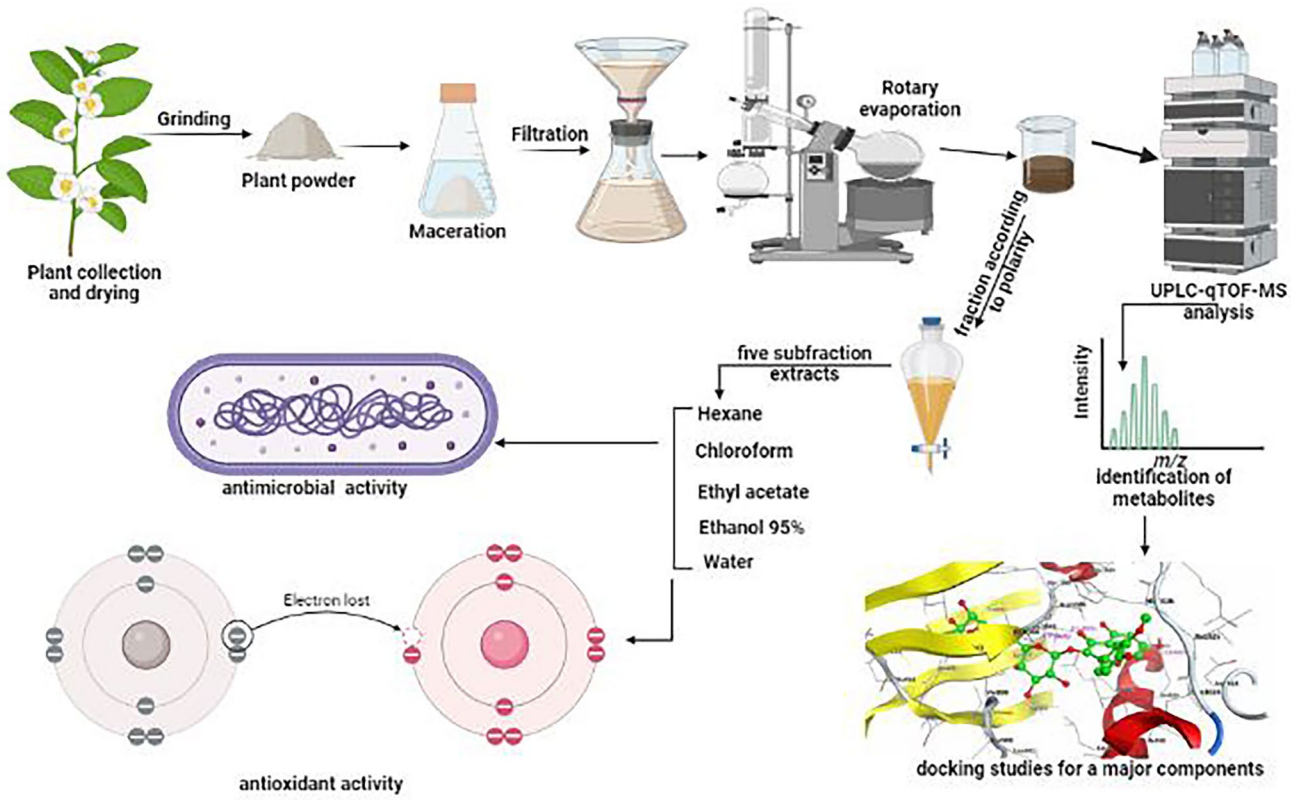
Received: 1 February 2024 / Accepted: 10 June 2024
Published online: 18 July 2024
© The Author(s) 2024 OPEN

Abstract
This study aimed to investigate the phytochemical constituents, antimicrobial activity, and antioxidant effects of successive extracts of *Ziziphora capitata* L. aerial parts. UPLC-QTOF-MS/MS identified 79 phytoconstituents, including phenolic acids, alkaloids, flavonoids, and anthocyanins, as major phytoconstituents. Additionally, primary phytochemical investigations revealed the presence of terpenoids, steroids, flavonoids, alkaloids, tannins, and saponins in various plant fractions. The MICs of successive extracts were tested against a range of microorganisms, including gram-positive bacteria (*Staphylococcus aureus, Bacillus subtilis, Streptococcus mutants, Enterococcus faecalis, Methicillin-Resistant Staphylococcus aureus* (MRSA) and *Staphylococcus epidermidis*), gram-negative bacteria (*Escherichia coli, Klebsiella pneumoniae, Pseudomonas aeruginosa, Salmonella typhimurium,* and *Enterobacter cloacae*), fungi (*Aspergillus niger* and *Penicillium aurantiogriseum*), and yeast (*Candida albicans* and *Candida tropicalis*), using the disk diffusion technique. The ethyl acetate and 95% ethanol extracts exhibited significant antibacterial activity against the tested microorganisms; however, the hexane fraction affected only *P. aeruginosa*. The effects of the $CHCl_3$ and H_2O fractions varied in their activities against most of the bacteria examined. Additionally, the AcOEt and 95% EtOH extracts exhibited significant antioxidant activity with $IC_{50} = 18.6 \pm 0.97$ and 30.4 ± 1.86 µg/mL, respectively, compared to that of ascorbic acid ($IC_{50} = 10.6 \pm 0.8$ µg/mL, reference drug). Antibacterial and antioxidant activities can be attributed to phytoconstituents, which were identified using UPLC-QTOF-MS/MS. Furthermore, docking simulations of the top ten phytochemicals of the 70% methanolic extract were carried out inside the active site of *S. aureus* DNA gyrase (PDB: 2XCT) and dihydropteroate synthase (DHPS) from *S. pneumoniae* (PDB: 2VEG) as bacterial targets and these compounds exhibited good binding modes with different types of interactions.

Supplementary Information The online version contains supplementary material available at https://doi.org/10.1007/s42452-024-06023-9.

✉ Youssif M. Youssif, youssif@drc.gov.eg; chemistyoussif@yahoo.com; ✉ Ahmed Ragab, Ahmed_ragab7@ymail.com; ahmed_ragab@azhar.edu.eg | [1]Medicinal and Aromatic Plants Department, Desert Research Center, Cairo 11753, Egypt. [2]Chemistry Department, Faculty of Science (Boys), Al-Azhar University, Nasr City, Cairo 11884, Egypt.

Graphical Abstract



Article Highlights

- *Ziziphora capitata* extracts have potential as natural antioxidants and antimicrobial agents.
- This study identified 79 phytochemicals, including anthocyanins, phenolic acids, alkaloids, flavonoids, terpenoids, and steroids.
- In silico docking simulations suggest that these phytochemicals could be used to develop innovative antibacterial agents.

Keywords *Ziziphora capitata* · Lamiaceae · UPLC-QTOF-MS/MS · Phytoconstituents · Flavonoids · Antimicrobial activity · Antioxidant · Molecular docking simulation

1 Introduction

As antibiotic resistance becomes an increasingly serious problem in medicine, there is an increasing interest in investigating medicinal plants as potential treatments [1]. Researchers want to create alternative medicines for treating antibiotic-resistant bacteria by harnessing the power of these natural substances [2]. Medicinal plants are important for healthcare worldwide, especially in countries with limited resources, where these plants serve as a primary source of healthcare for approximately 80% of the population [3]. Abundant in bioactive compounds, medicinal plants have been extensively employed in traditional medicine to address a wide spectrum of ailments [4, 5]. In the pursuit of identifying antimicrobial agents that are both safe and efficacious while minimizing undesirable side effects, researchers have turned to ethnobotanical methodologies [6]. By exploring the potential of plants used in conventional and alternative medicine,

these methodologies offer avenues for the discovery of novel therapeutic agents [3, 6]. The Lamiaceae, often known as the Labiatae family, is a large assemblage of flowering plants found around the world, with 236 genera and about 6900–7200 species [7]. The genus Ziziphora is a widely recognized member of this family, with applications in pharmacy, chemistry, medicine, traditional medicine, and folk remedies [8]. *Ziziphora capitata* L. is an edible plant that has also historically been used to treat a wide range of conditions such as hypertension, insomnia, neurasthenia, tracheitis, heart and coronary artery disorders, lung abscess, high temperature, edema, and hemorrhoids [9]. Besides, *Z. capitata* has antibacterial, antioxidant, and cytotoxic effects [10, 11]. The results obtained from the previous study on *Z. capitata* L. in Iran exhibited potency against *Escherichia coli*, *Staphylococcus aureus*, *Staphylococcus epidermidis*, *Salmonella typhi*, and *Pseudomonas aeruginosa* [12]. Molecular docking is an essential tool in computer-assisted drug design and structural molecular biology [13], where it aims to predict the interaction between the designed compound and the enzyme and the possible binding site and strength of the interactions. Therefore, these results help to provide insight into the mechanism of action and therapeutic potential of the drug [14]. The goal of this study was to identify phytoconstituents in *Z. capitata* through docking studies of major components as well as antimicrobial and antioxidant activity assessments of subsequent fractions of *Ziziphora capitata* L.

2 Materials and methods

2.1 Plant materials

The aerial parts of the wild plant *Ziziphora capitata* L (Lamiaceae) were collected during the flowering stage (February 2020) from Wadi Hala'zeen (31°25′21.9"N and 26°51′41.6"E), located in the Marsa Matrouh, Governorate of Egypt. All plant collection methods agreed to a rule created in the United States by the Plant Conservation Roundtable, Washington, D.C., June 18, 1986, this policy is called BOTANY 440/540. The plant was identified by Dr. Atia Eisa, a plant taxonomy lecturer at the Faculty of Science, Damanhur University. The identification was further verified by Dr. Adel El-Gazar, a plant taxonomist professor et al.-Arish University, according to [15, 16]. A voucher herbarium specimen was deposited in the herbarium of the Desert Research Center (CAIH) with code number CAIH-1251-R. After collection, the Z. *capitata* L. plant was stored in a shaded area to protect it from direct sunlight, insects, and predators. The plant samples were then thoroughly cleaned to remove any dirt particles and shade dried until a constant weight was achieved. Once dried, the plant material was ground into a fine powder to facilitate chemical analysis.

2.2 Extraction procedure

A 70% methanol (MeOH) solution was used as the solvent to extract the chemical profile of *Z. capitata* L. Air-dried plant-based powder (2 g) was mixed with 10 mL of the solvent in an ultrasonic water bath for 30 min before analysis using UPLC-QTOF-MS/MS. The extract was then filtered to remove any debris using a 22-m Millipore filter. For the antimicrobial assay, 20 g of air-dried *Z. capitata* L. powder was extracted using organic solvents in increasing order of polarity, including, hexane, chloroform ($CHCl_3$), ethyl acetate (AcOEt), 95% ethanol (EtOH), and H_2O. The weight of each solvent residue was calculated and recorded after drying [17].

2.3 Preliminary phytochemical screening

Testing for flavonoids and glycosides and/or carbohydrates according to [18], saponin and alkaloids (Dragendorff's test) methods described by [19], steroids, and/or terpenes was performed as [20]. It is a useful tool for detecting the presence of different classes of chemical compounds in plant extracts, but it only provides a broad indication of the types of compounds present to obtain a more detailed understanding of the chemical composition of the extract.

2.4 Metabolites analysis via UPLC-QTOF-MS/MS

The Proteomics and Metabolomics Lab at Cancer Children Hospital 57,357 in Cairo, Egypt, used Sciex Exion LFC separation chromatography with a TripleTOF 5600 + and an Xbridge C18 column to analyze metabolites from a *Z. capitata* L. extract. The lab used specific parameter settings to detect and record the product ions and UPLC-QTOF-MS/MS in positive ion mode. Chemical identification was done by comparing masses and fragmentation patterns with previously reported

compounds and using databases such as the HMDB and NIST. MS-DIAL 3.52 software was used to analyze the data, and peaks were identified from the total ion chromatogram (TIC) using Master View software. Metabolites were identified by comparing retention time and MS data, including isotopic distribution, precise mass, and fragmentation patterns in positive ionization modes. Identification was validated by cross-referencing with a plant lexicon and literature. The resulting data matrices were imported into Microsoft Excel, and the metabolite data were standardized by weight and internal standard normalization [11, 17].

2.5 Antimicrobial activity assay

The microbial strains used in this study were obtained from the Regional Center for Mycology and Biotechnology (RCMB) culture collection et al.-Azhar University, Cairo, Egypt. In this study, we evaluated the antibacterial profile of compounds against various bacterial and fungal species using a modified well diffusion method. Microbial samples were cultured and placed on agar plates. The antimicrobial activity was evaluated by applying 100 mL of each tested sample at a concentration of 10 mg/mL to 6 mm diameter holes punched in the agar gel. The plates were incubated, and the inhibition zones were measured to determine the antimicrobial activity. The study used negative and positive controls, and the MIC of the active samples was determined using the broth microdilution method. The lowest concentration of the sample that completely inhibited the growth of the microorganisms was recorded as the MIC after incubation [21].

2.6 Antioxidant assay

The 2,2-diphenyl-1-picrylhydrazyl (DPPH) radical was freshly generated in a 0.004% w/v MeOH solution, which was then kept at 10 °C in the dark. The test chemical was produced as a MeOH solution. To 3 ml of DPPH solution, a 40 µl aliquot of the MeOH solution was added. Absorbance measurements were taken immediately using a UV– visible spectrophotometer (Milton Roy, Spectronic 1201). Data were acquired every minute until the absorbance stabilized (16 min), and the decline in absorbance at 515 nm was continually monitored. The absorbances of the reference molecule ascorbic acid and the DPPH radical without an antioxidant (control) were also measured. All calculations were performed in triplicate and averaged [22]. The following formula was used to determine the percentage inhibition (PI) of the DPPH radical:

$$\mathrm{PI} = \left[\{(AC - AT)/AC\} \times 100\right]$$

where *AC* = Absorbance of the control at t = 0 min and *AT* = absorbance of the sample plus DPPH at t = 16 min. Graphpad Prism software (San Diego, CA, USA) was used to determine the 50% inhibitory concentration (IC_{50}), which is the concentration needed to achieve 50% DPPH radical scavenging activity, using graphic plots of the dose response curve.

2.7 Molecular docking simulations

The docking simulation process was performed using Molecular Operating Environmental Software (MOE) [23–25] for the top ten compounds in methanolic extract for *Z. capitata* L. in positive ionization mode. It was performed inside the active *S. aureus* DNA gyrase (PDB: 2XCT) and dihydropteroate synthase (DHPS) from Streptococcus pneumonia (PDB: 2VEG) [26–28]. The structure of the top ten compounds in the methanolic extract of *Z. capitata* L. was built using Chembiodraw 2014 and converted as a smile code, then exported to MOE software as described previously [29–31]. The structure of the tested compounds was subjected to hydrogen bonds and energy minimization under default parameters and saved as an mdb file.

3 Results and discussion

3.1 Preliminary phytochemical screening

Successive extracts of *Z. capitata* L. contain flavonoids, carbohydrates and/or glycosides, sterols and/or terpenes, and saponins. The presence of carbohydrates and/or glycosides was detected in the 95% EtOH and H2O fractions, where sterols and/or terpenes were detected in the hexane and CHCl3 fractions, while flavonoids were present in the AcOEt,

Table 1 Phytochemical analysis of successive extracts of *Z. capitata* L. aerial parts

Test	Hexane	CHCl3	AcOEt	95% EtOH	H2O
Flavonoids	–	–	+	+	+
Alkaloids	–	–	–	–	–
Glycosides and / or carbohydrates	–	–	–	+	+
Sterols and / or terpenens	+	+	–	–	–
Saponins	–	–	+	+	+

(+) mean present, (–) mean absent

95% EtOH, and H2O fractions. No alkaloids were detected in all extracts, while saponins present in AcOEt, 95% EtOH, and H2O fractions Table 1.

3.2 Metabolites of *Z.* capitata L. using UPLC-QTOF-MS/MS analysis

The metabolite composition of the *Z. capitata* L. aerial part was studied using UHPLC-QTOF-MS/MS in positive ionization mode. The findings revealed 78 metabolites, including phenolic acids, alkaloids, anthocyanidins, and mostly flavonoids, as indicated in Table 2, Table S1 and Fig. 1. Previous research on other Ziziphora species has been consistent with the chemical analysis of *Z. capitata* L. extract, which revealed that flavonoids are the most abundant components. The major compounds detected were baicalein-7-*O*-glucuronide, α aminoisobutyrate, and pelargonidin-3-*O*-glucoside, which were calculated as 561,443.750 µg/g, 520,653.656 µg/g, and 338,118.781 µg/g, respectively. Flavonoids, including flavones, flavonols, and flavanones, as well as their conjugates, *O*-glycosides, were detected in the plant extract using UPLC-QTOF-MS/MS. The MS analysis also indicated the existence of different sugars, which were recognized by their varied *m/z* ratios. For example, a loss of 132 amu indicated the existence of a pentose sugar, whereas a loss of 146 amu indicated the presence of a monodeoxyhexose sugar. Similarly, a loss of 162 amu indicated the presence of hexose sugar, whereas a loss of 176 amu indicated the presence of hexuronic acid residue. The *m/z* ratios of the ions generated during MS allowed the identification of the types of sugars contained in the sample [17].

3.2.1 Phenolic compounds

Phenolic acids were also detected among the compounds, including chlorogenic acid, which was identified by its *m/z* of 355.097 and detected at Rt 6.426 min peak (33). Fragment ions *m/z* 181 at Rt 6.166 min peak (28) corresponding to caffeic acid. Therefore, chlorogenic acid and caffeic acid was confirmed based on the presence of fragment ions.

3.2.2 Flavonoid compounds

For C-glycosides, luteolin-6-C-glucoside with *m/z* 449.107 and molecular formula ($C_{21}H_{21}O_{11}$) as in peak (27), revealed losses of 162 amu (-hexose unit), and vitexin-2″-*O*-rhamnoside with *m/z* 579.165 and molecular formula ($C_{27}H_{30}O_{16}$) as in peak (55), fragmentation revealed losses of 146 amu (-monodeoxyhexose unit). For *O*-glucoside, isorhamnetin-3-*O*-glucoside with *m/z* 479.114 and molecular formula ($C_{22}H_{22}O_{12}$) were detected in peak 50, showing losses of (162 amu)-hexose unit, identified as isorhamnetin-3-*O*-glucoside, where isorhamnetin-3-*O*-rutinoside with *m/z* 625.163 and molecular formula ($C_{28}H_{32}O_{11}$) as in peak (42) fragmentation revealed losses of 308 amu (-hexose unit and—monodeoxyhexose). Fragmentation of baicalein-7-*O*-glucuronide with *m/z* 477.092 and molecular formula ($C_{21}H_{18}O_{11}$) as in peak (59) revealed losses of 176 amu (-hexouronic acid unit). Acacetin-7-*O*-rutinoside with *m/z* 593.187 with molecular formula ($C_{28}H_{32}O_{14}$) was detected at Rt 9.370 min and its aglycone (acacetin) with *m/z* 285.084 with molecular formula ($C_{16}H_{12}O_5$) was detected at Rt 7.774 min, respectively, peak fragmentation pattern (63) revealed losses of 162 amu (-hexose unit) and losses of 146 amu (-monodeoxyhexose), identified as acacetin-7-*O*-rutinoside. Others, diosmin with *m/z* 609.183 and molecular formula ($C_{28}H_{32}O_{15}$) detected at Rt 7.812 as in peak (48), fragmentation revealed losses of 308 amu (-hexose unit and -monodeoxyhexose unit).

Table 2 Compound name in MeOH extract (70%) for *Z. capitata* L. via UPLC-QTOF-MS/MS in positive ionization mode

No.	Rt	*m/z*	Formula	Name of compound	$[M+H]^+$	Height	Ontology	MS
1	1.11	110.009	C_6H_7NO	4-Aminophenol	$[M+H]^+$	62,673.445	Anilines	66, 68, 110
2	1.275	104.107	$C_4H_9NO_2$	*α*-Aminoisobutyrate	$[M+H]^+$	520,653.66	*α* amino acids	58, 59, 60, 104
3	1.34	176.008	$C_{10}H_9NO_2$	*β*-Indoleacetic acid	$[M+H]^+$	7038.222	Indole-3-acetic acid	130, 158, 176
4	1.365	140.071	$C_6H_5NO_3$	6-Hydroxynicotinic acid	$[M+H]^+$	9085.777	Pyridine carboxylic acids	96, 140
5	1.377	365.105	$C_{10}H_{13}N_4O_9P$	Xanthosine-5′ monophosphate	$[M+H]^+$	105,939.66	Purine ribonucleoside monophosphates	185, 203, 236, 365
6	1.377	175.053	$C_6H_6O_6$	cis-Aconitate	$[M+H]^+$	9967.444	Tricarboxylic acids	70, 86, 129, 175
7	1.39	335.075	$C_{11}H_{15}N_2O_8P$	*β* -Nicotinamide mononucleotide	$[M+H]^+$	13,492.888	Nicotinamide nucleotides	215, 227, 289, 335
8	1.428	116.07	$C_5H_9NO_2$	L-Proline	$[M+H]^+$	147,703.33	Proline and derivatives	70, 116
9	1.428	130.09	$C_6H_{11}NO_2$	L- *β* –Homoproline	$[M+H]^+$	28,086.111	Pyrrolidines	56, 70, 84, 112, 130
10	1.454	136.06	$C_5H_5N_5$	Adenine	$[M+H]^+$	9925.888	6-Aminopurines	77, 92, 109, 119, 136
11	1.48	268.981	$C_8H_{16}N_2O_4S_2$	DL-Homocystine	$[M+H]^+$	14,594.777	*α* amino acids	137, 251, 268, 269
12	1.48	289.089	$C_{15}H_{12}O_6$	3′, 4′, 5, 7, Tetrahydroxyflavanone	$[M+H]^+$	4495.777	Flavanones	274, 289
13	1.48	229.155	$C_{14}H_{12}O_3$	Resveratrol	$[M+H]^+$	3528.888	Stilbenes	70, 117, 142, 177, 229
14	1.517	215.049	$C_{13}H_{14}N_2O$	Harmaline	$[M+H]^+$	15,447.333	Harmala alkaloids	126, 215
15	1.91	130.05	$C_5H_7NO_3$	L-5-Oxoproline	$[M+H]^+$	48,279.667	*α* amino acids	56, 70, 84, 130
16	1.91	86.059	C5H11N	Piperidine	$[M+H]^+$	10,884.888	Piperidines	56, 57, 85, 86
17	1.924	268.104	$C_{10}H_{13}N_5O_4$	Adenosine	$[M+H]^+$	28,142.777	Purine nucleosides	136, 268
18	2.349	166.085	$C_9H_{11}NO_2$	L-(-)-Phenylalanine	$[M+H]^+$	45,858.667	Phenylalanine	80, 120, 148, 166
19	4.403	447.149	$C_{22}H_{22}O_{10}$	Sissotrin	$[M+H]^+$	1750.444	Isoflavonoid-*O*-glycosides	163, 186, 285, 325, 343, 447
20	4.928	457.145	$C_{17}H_{21}N_4O_9P$	Riboflavin5 monophosphate sodium salt	$[M+H]^+$	15,174.666	Flavin nucleotides	373, 457
21	4.967	169.083	$C_5H_4N_4O_3$	Uric acid	$[M+H]^+$	2272.222	Xanthines	115, 168, 169
22	5.441	411.165	$C_{28}H_{42}O_2$	*γ* –Tocotrienol	$[M+H]^+$	9911.333	Tocotrienols	411
23	5.52	481.138	$C_{21}H_{20}O_{13}$	Gossypin	$[M+H]^+$	1659.111	Flavonoid-8-*O*-glycosides	170, 481
24	5.816	417.056	$C_{21}H_{20}O_9$	Daidzein-8-C-glucoside	$[M+H]^+$	14,781.222	Isoflavonoid C-glycosides	415, 417
25	6.026	162.054	$C_9H_7NO_2$	1H-indole-3-carboxylic acid	$[M+H]^+$	15,934	Indole carboxylic acids	63, 65, 89, 91, 116, 117, 118, 144, 162
26	6.127	124.076	$C_6H_5NO_2$	Isonicotinate	$[M+H]^+$	2387.111	Pyridine carboxylic acids	80, 96
27	6.154	449.107	$C_{21}H_{20}O_{11}$	Luteolin-6-C-glucoside	$[M+H]^+$	9788.333	Flavonoid C-glycosides	299, 329, 353, 413, 431, 449
28	6.166	181.085	$C_9H_8O_4$	Caffeic acid	$[M+H]^+$	10,068.333	Hydroxycinnamic acids	68, 79, 91, 135, 163, 181
29	6.166	163.074	$C_6H_{14}N_2O_3$	DL-5-Hydroxylysine	$[M+H]^+$	5805.444	Alpha amino acids	79, 91, 132, 135, 145, 163
30	6.193	611.15	$C_{27}H_{31}O_{16}$	Delphinidin-3-O-(6″-*O*-alpha-rhamnopyranosyl-beta glucopyranoside)	$[M+H]^+$	2137.555	Anthocyanidin-3-*O*-glycosides	303, 356, 465, 611
31	6.206	303.05	$C_{15}H_{10}O_7$	Quercetin	$[M+H]^+$	2183.666	Flavonols	162, 286, 303
32	6.244	579.183	$C_{30}H_{26}O_{12}$	Procyanidin B2	$[M+H]^+$	21,027	Biflavonoids and polyflavonoids	579
33	6.426	355.097	$C_{16}H_{18}O_9$	Chlorogenic acid	$[M+H]^+$	5224.111	Quinic acids and derivatives	137, 145, 155, 163, 174, 179, 191, 197, 337, 355

Table 2 (continued)

No.	Rt	*m/z*	Formula	Name of compound	$[M+H]^+$	Height	Ontology	MS
34	6.773	611.164	$C_{27}H_{30}O_{16}$	Rutin	$[M+H]^+$	30,001.222	Flavonoid-3-O-glycosides	303, 465, 611
35	6.816	595.156	$C_{27}H_{30}O_{15}$	Datiscin	$[M+H]^+$	6930.666	Flavonoid-3-*O*-glycosides	287, 317, 449, 463, 595
36	6.994	139.11	$C_6H_6N_2O_2$	Urocanic acid	$[M+H]^+$	6082.555	Imidazolyl carboxylic acids and derivatives	65, 93, 121, 139
37	7.021	741.228	$C_{33}H_{40}O_{19}$	Kaempferol-3-*O*-robinoside-7-*O*-rhamnoside	$[M+H]^+$	7491.666	Flavonoid-7-*O*-glycosides	287, 449, 595, 741
38	7.089	595.163	$C_{27}H_{31}O_{15}$	Pelargonidin-3,5-di-*O*-glucoside	$[M+H]^+$	19,208.445	Anthocyanidin-5-*O*-glycosides	271, 287, 433, 595
39	7.128	465.102	$C_{21}H_{20}O_{12}$	Hyperoside	$[M+H]^+$	14,143.333	Flavonoid-3-*O*-glycosides	303, 362, 432, 448, 465
40	7.155	241.083	$C_6H_{12}N_2O_4S_2$	L-Cystine	$[M+H]^+$	6977	L-Cysteine-S-conjugates	161, 223, 241
41	7.358	336.126	$C_{15}H_{21}N_5O_4$	N-6-(δ -2-Isopentenyl) adenosine hemihydrate	$[M+H]^+$	1803	Purine nucleosides	146, 230, 276, 336
42	7.511	625.163	$C_{28}H_{32}O_{16}$	Isorhamnetin-3-*O*-rutinoside	$[M+H]^+$	15,018.888	Flavonoid-3-*O*-glycosides	317, 479, 625
43	7.685	137.097	$C_{10}H_{16}$	Sabinene	$[M+H]^+$	6556.444	Bicyclic monoterpenoids	77, 79, 104, 107, 118, 121, 122, 135, 137
44	7.698	133.102	C_9H_8O	Cinnamaldehyde	$[M+H]^+$	10,556.111	Cinnamaldehydes	65, 77, 79, 91, 103, 105, 115, 117, 133
45	7.761	449.104	$C_{21}H_{21}O_{11}$	Cyanidin-3-glucoside	$[M+H]^+$	4070.777	Anthocyanidin-3-*O*-glycosides	287, 449
46	7.761	287.057	$C_{15}H_{10}O_6$	Luteolin	$[M+H]^+$	3467.111	Flavones	153, 167, 195, 269, 287
47	7.774	285.084	$C_{16}H_{12}O_5$	Acacetin	$[M+H]^+$	1669.555	4′-*O*-Methylated flavonoids	95, 125, 157, 165, 242, 270, 285
48	7.812	609.183	$C_{28}H_{32}O_{15}$	Diosmin	$[M+H]^+$	26,451	Flavonoid-7-*O*-glycosides	301, 463, 609
49	7.876	579.091	$C_{27}H_{30}O_{14}$	Rhoifolin	$[M+H]^+$	5968.333	Flavonoid-7-*O*-glycosides	271, 433, 579
50	7.888	479.114	$C_{22}H_{22}O_{12}$	Isorhamnetin-3-*O*-glucoside	$[M+H]^+$	10,010.222	Flavonoid-3-*O*-glycosides	303, 317
51	7.947	433.11	$C_{21}H_{21}O_{10}$	Pelargonidin-3-*O*-glucoside	$[M+H]^+$	338,118.78	Anthocyanidin-3-*O*-glycosides	271, 433
52	8.048	409.163	$C_{24}H4_0O_5$	Cholic acid	$[M+H]^+$	29,393.554	Trihydroxy bile acids	391, 409
53	8.148	179.109	$C_9H_6O_4$	Daphnetin	$[M+H]^+$	12,994.444	7,8-Dihydroxycoumarins	133, 161, 179
54	8.148	595.186	$C_{27}H_{30}O_{15}$	Apigenin-6-C-glucoside -7-*O*-glucoside	$[M+H]^+$	1963.777	Flavonoid-7-*O*-glycosides	279, 577, 595
55	8.199	579.165	$C_{27}H_{30}O_{14}$	Vitexin-2″-*O*-rhamnoside	$[M+H]^+$	3893.555	Flavonoid 8-C-glycosides	397, 415, 417, 433, 579
56	8.288	493.166	$C_{23}H_{25}O_{12}$	Malvidin-3-galactoside	$[M+H]^+$	3249.666	Anthocyanidin-3-*O*-glycosides	297, 317, 321, 331, 493
57	8.376	361.096	$C_{18}H_{16}O_8$	Rosmarinic acid	$[M+H]^+$	224,702.67	Coumaric acids and derivatives	117, 145, 163, 181, 211, 361
58	8.4	146.063	C_9H_7NO	3-Formylindole	$[M+H]^+$	28,522.666	Indoles	91, 118, 146
59	8.537	447.092	$C_{21}H_{18}O_{11}$	Baicalein-7-*O*-glucuronide	$[M+H]^+$	561,443.75	Flavonoid-7-*O*-glucuronides	271, 447
60	8.537	271.062	$C_{15}H_{10}O_5$	Apigenin	$[M+H]^+$	8489.444	Flavones	91, 119, 153, 271
61	8.948	153.122	$C_8H_8O_3$	*o*- methoxybenzoic acid	$[M+H]^+$	2114.222	Methoxy benzoic acids and derivatives	53, 91, 135, 153
62	9.275	463.085	$C_{21}H_{18}O_{12}$	Kaempferol-3-Glucuronide	$[M+H]^+$	36,892.667	Flavonoid-3-*O*-glucuronides	287, 463
63	9.37	593.187	$C_{28}H_{32}O_{14}$	Acacetin-7-*O*-rutinoside	$[M+H]^+$	79,591.89	Flavonoid-7-*O*-glycosides	285, 447, 593
64	9.622	193.12	$C_{10}H_8O_4$	Scopoletin	$[M+H]^+$	3156.555	7-Hydroxy coumarins	91, 193
65	9.622	211.132	$C_{12}H_{18}O_3$	(+-)-Jasmonic acid	$[M+H]^+$	2737.555	Jasmonic acids	196, 211
66	9.686	595.142	$C_{30}H_{26}O_{13}$	Kaempferol-3-*O*-(6-p-coumaroyl)-glucoside	$[M+H]^+$	10,787.555	Flavonoid 3-*O*-p-coumaroyl glycosides	119, 147, 271, 313, 595

Table 2 (continued)

No.	Rt	*m/z*	Formula	Name of compound	$[M+H]^+$	Height	Ontology	MS
67	9.918	137.133	$C_5H_4N_4O$	Hypoxanthine	$[M+H]^+$	1959.222	Hypoxanthines	78, 137
68	10.349	606.258	$C_{16}H_{25}N_5O_{16}P_2$	Guanosine 5′-diphosphate-D-mannose	$[M+H]^+$	2866.777	Purine nucleotide sugars	606
69	11.11	305.116	$C_{15}H_{12}O_7$	(+-)-Taxifolin	$[M+H]^+$	3042.111	Flavanonols	288, 305
70	11.559	301.07	$C_{16}H_{12}O_6$	3, 5, 7,-Trihydroxy-4′- methoxyflavone	$[M+H]^+$	101,540.34	Flavonols	229, 258, 285, 286, 301
71	12.333	163.112	$C_{10}H_{14}N_2$	Nicotine	$[M+H]^+$	3925.111	Pyrrolidinylpyridines	80, 84, 106, 115, 117, 120, 130, 132, 135, 145, 163
72	14.392	387.175	$C_{17}H_{22}O_{10}$	1-*O*-*β*-D-glucopyranosyl sinapate	$[M+H]^+$	39,099.777	Hydroxycinnamic acid glycosides	93, 105, 119, 129, 387
73	16.435	191.105	$C_7H_{14}N_2O_4$	DL-*α*-Diaminopimelic acid	$[M+H]^+$	5037.111	*α* amino acids	191
74	19.426	123.114	$C_6H_6N_2O$	Nicotinamide	$[M+H]^+$	2187.333	Nicotinamides	78, 123
75	20.302	149.022	$C_9H_8O_2$	trans-Cinnamate	$[M+H]^+$	49,419.222	Cinnamic acids	65, 73, 80, 91, 93, 121, 131, 149
76	20.315	317.114	$C_{16}H_{12}O_7$	3, 3′, 4′, 5,-Tetrahydroxy-7-methoxyflavone	$[M+H]^+$	15,887.777	Flavonols	207, 264, 282. 317
77	23.041	175.149	$C_6H_{14}N_4O_2$	L-Arginine	$[M+H]^+$	1482.444	L-*α*-amino acids	118, 175
78	26.934	118.085	$C_5H_{11}NO_2$	Glycine Betaine	$[M+H]^+$	5204.111	*α* amino acids	58, 59, 72, 118

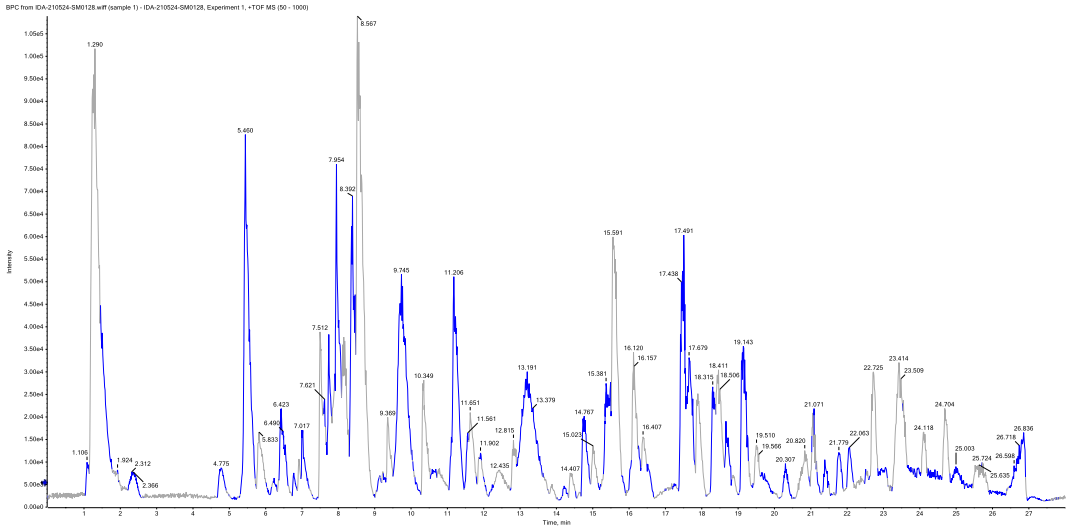


Fig. 1 TIC of total ion chromatogram for UPLC-QTOF-MS/MS in Positive -mode

3.2.3 Anthocyanin's compounds

Anthocyanins were also detected as another class of compounds present in the plant extracts, delphinidin-3-*O*-(6″-*O*-*α* -rhamnopyranosyl-*β* glucopyranoside), which had a molecular weight *m/z* 611.150 and a molecular formula of $C_{27}H_{31}O_{16}$, and was detected at Rt of 6.193 min. Fragmentation of this compound showed losses of 162 amu and 146 amu, thereby confirming its identity as delphinidin-3-*O*-(6″-*O*- *α* -rhamnopyranosyl- *β* -glucopyranoside). Cyanidin-3-glucoside, with a molecular weight of 449.104 and a molecular formula of $C_{21}H_{21}O_{11}$, was detected at Rt 7.761 min. The fragmentation showed losses of 162 amu, thereby confirming its identity as cyanidin-3-glucoside. Pelargonidin-3,5-di-*O*-glucoside with *m/z* 595.163 and molecular formula ($C_{27}H_{31}O_{15}$) detected at Rt 7.089 min and pelargonidin-3-*O*-glucoside with *m/z* 433.110 and molecular formula ($C_{21}H_{21}O_{10}$) detected at Rt 7.947 min peak (51), fragmentation pattern revealed losses of 324 amu (-2 hexose unit) and losses of 162 amu, identified as pelargonidin-3,5-di-*O*- glucoside and pelargonidin-3-*O*-glucoside, respectively.

3.2.4 Other compounds

Pyridine carboxylic acids were found to be 6-hydroxynicotinic acid with *m/z* 140.071 and the molecular formula ($C_6H_5NO_3$) at Rt 1.365 min. Fragmentation of this compound revealed losses of 44 amu (–CO_2), validating its identification as 6-hydroxynicotinic acid. The *m/z* of xanthosine-5′-monophosphate was 365.105, and the chemical formula was $C_{10}H_{13}N_4O_9P$, Peak (5) was discovered at Rt of 1.377 min. Fragmentation of this compound revealed losses of 81 amu (–H_2O_4P-) and 162 amu, confirming its identification as xanthosine-5′-monophosphate. Hydroxycoumarins such as daphnetin and scopoletin were detected in the plant sample at Rt 8.148 min and Rt 9.622 min these chemicals may contribute to the plant's increased antibacterial activity [32].

3.3 Biological activity

The zone of inhibition ranged from 8.20 to 15.17 mm against all tested Gram-positive and Gram-negative cells, as indicated in Table 3. The AcOEt extract demonstrated antimicrobial activity against most of the tested strains, with the highest inhibition zones of 13.93, 9.93, 9.13, 11.13, 12.97, 12.03, and 9.42 mm observed against *S. aureus*, *S. mutants, E. faecalis*, *E. coli*, *P. aeruginosa, S. typhimurium*, and *E. cloacae,* respectively. Ethanol 95% extract exhibited potent antibacterial activity against six of the tested strains, with the highest inhibition zones of 10.13, 8.20, 9.97, 10.13, 10.87, and 8.64 mm against *S. aureus*, *E. faecalis*, *E. coli*, *P. aeruginosa, S. typhimurium*, and *E. cloacae,* respectively. H2O extract exhibited antibacterial activity against four of the tested strains of gram-negative bacteria only, with the highest inhibition zones of 10.13, 15.17, 11.93 and 9.18 mm against *E. coli*, *K. pneumoniae, S. typhimurium*, and *E. cloacae,* respectively. Chloroform extract exhibited potent antimicrobial activity against two tested strings of Gram negatvie bacteria only, with the highest

Table 3 Inhibition zone (mm) of different plant fractions on tested bacteria and fungi

Tested microorganism	Hexane	CHCl3	AcOEt	95% EtOH	H2O	Control
Gram positive bacteria						*Gentamycin*
Staphylococcus aureus (RCMB010010)	NA	NA	13.93±0.12	10.13±0.15	NA	24.01±0.01
Bacillus subtilis RCMB 015 (1) NRRL B-543	NA	NA	NA	NA	NA	26.02±0.03
Streptococcus mutants RCMB 017 (1) ATCC 25175	NA	NA	9.93±0.12	NA	NA	20.01±0.02
Enterococcus faecalis (ATCC 29212)	NA	NA	9.13±0.15	8.20±0.26	NA	26.09±0.01
Methicillin-Resistant Staphylococcus aureus (MRSA)	NA	NA	NA	NA	NA	15.00±0.5
Staphylococcus epidermidis RCMB 009(2)	NA	NA	NA	NA	NA	28.03±0.5
Gram negatvie bacteria:						*Gentamycin*
Escherichia coli (RCMB 010052) ATCC 25955	NA	8.97±0.15	11.13±0.15	9.97±0.06	10.13±0.15	29.90±0.01
Klebsiella pneumonia RCMB 003 (1) ATCC 13883	NA	NA	NA	NA	15.17±0.15	21.01±0.04
Pseudomonas aeruginosa ATCC 27853	12.07±0.12	10.93±0.21	12.97±0.15	10.13±0.12	NA	17.00±0.01
Salmonella typhimurium RCMB 006 (1) ATCC 14028	NA	NA	12.03±0.15	10.87±0.15	11.93±0.12	17.02±0.03
Enterobacter cloacae RCMB 001 (1) ATCC 23355	NA	NA	9.42±0.26	8.64±0.18	9.18±0.38	30.07±0.51
Fungi						*Ketoconazole*
Aspergillus niger RCMB 002005)	NA	NA	NA	NA	NA	15.07±0.06
Penicillium aurantiogriseum IMI 89372	NA	NA	NA	NA	NA	25.00±0.50
Yeast						*Ketoconazole*
Candida albicans RCMB 005003 (1) ATCC 10231	NA	NA	NA	NA	NA	20.03±0.04
Candida tropicalis RCMB 005004 (1)	NA	NA	NA	NA	NA	21.00±0.5

NA: No activity. The sample was tested at 10 mg/mL concentration. The test was done using disk diffusion technique, Well diameter: 6.0 mm (100 µl was tested)

inhibition zones of 8.97 and 10.93 mm against *E. coli* and *P. aeruginosa*, respectively. The hexane extract showed potent antimicrobial activity against only one tested strain of Gram- negative bacteria, with the highest inhibition zone of 12.07 mm observed against *P. aeruginosa*. The hexane, CHCl3, and H2O fractions obtained through successive extractions showed no inhibitory effect on any of the tested gram-positive bacteria. Similarly, all successive fractions showed no inhibitory effect on any of the tested fungi and yeast strains. The most effective extracts, including the AcOEt, 95% EtOH, and H2O of *Z. capitata* L., were evaluated for their minimum inhibitory concentration (MIC) against *S. aureus*, *S. mutants, E. faecalis*, *E. coli*, *K. pneumoniae, P. aeruginosa, S. typhimurium*, and *E. cloacae*. The MIC values of the EtOH fraction varied from 2500 to 10,000 µg/ mL, whereas the MIC values of the 95% EtOH extract ranged from 5000 to 10,000 µg/mL, and the MIC values of the H2O extract varied from 2500 to 10,000 µg/mL. According to the results shown in Table 4, the AcOEt extract exhibited the lowest MIC against *S. aureus* and *P. aeruginosa,* whereas the H2O extract showed the lowest MIC activity against *K. pneumoniae*.

Table 4 MIC (µg/mL) of different plant fractions on tested bacteria

Tested microorganism	AcOEt	95% EtOH	H2O
Gram positive bacteria			
Staphylococcus aureus (RCMB010010)	2500	5000	–
Streptococcus mutants RCMB 017 (1) ATCC 25175	5000	–	–
Enterococcus faecalis (ATCC 29212)	5000	10,000	–
Gram negatvie bacteria			
Escherichia coli (RCMB 010052) ATCC 25955	5000	5000	5000
Klebsiella pneumonia RCMB 003 (1) ATCC 13883	–	–	2500
Pseudomonas aeruginosa ATCC 27853	2500	5000	–
Salmonella typhimurium RCMB 006 (1) ATCC14028	5000	5000	5000
Enterobacter cloacae RCMB 001 (1) ATCC 23355	10,000	10,000	10,000

Table 5 Scavenging activity of successive extracts of *Z. capitata* L. against (DPPH)

Conc. µg/mL	Hexane	$CHCl_3$	AcOEt	95% EtOH	H_2O	Ascorbic acid
1280	56.08 ± 3.74	68.23 ± 2.79	97.14 ± 0.28	96.03 ± 0.29	94.57 ± 0.39	98.91 ± 0.74
640	28.71 ± 1.93	51.39 ± 2.27	95.73 ± 0.29	94.16 ± 0.32	83.21 ± 0.67	97.83 ± 0.39
320	20.48 ± 1.06	29.14 ± 1.92	94.07 ± 0.61	92.83 ± 0.15	77.15 ± 1.43	95.64 ± 1.22
160	9.83 ± 0.71	18.75 ± 1.34	92.78 ± 0.34	91.06 ± 0.22	58.48 ± 2.68	92.31 ± 0.87
80	4.31 ± 0.58	9.24 ± 0.62	91.56 ± 0.62	89.64 ± 0.48	31.98 ± 2.34	90.25 ± 0.41
40	1.89 ± 0.43	5.17 ± 0.59	87.21 ± 1.03	60.76 ± 1.92	20.72 ± 1.62	83.09 ± 1.95
20	0.67 ± 0.29	3.28 ± 0.34	53.09 ± 1.85	38.32 ± 1.64	9.86 ± 0.52	71.38 ± 1.39
10	0.32 ± 0.14	1.76 ± 0.18	30.75 ± 0.97	19.63 ± 0.59	5.18 ± 0.73	48.52 ± 2.64
5	0.14 ± 0.08	0.85 ± 0.21	14.93 ± 0.15	10.48 ± 0.34	2.91 ± 0.58	40.36 ± 0.82
2.5	0.05 ± 0.03	0.49 ± 0.35	8.24 ± 0.38	6.17 ± 0.29	0.87 ± 0.39	34.57 ± 0.79
IC_{50} µg/mL	1137.8 ± 39.72	620 ± 18.46	18.6 ± 0.97	30.4 ± 1.86	134.4 ± 2.94	10.6 ± 0.8

3.4 Antioxidant activities

The results of DPPH scavenging activity of five successive extracts (hexane, CHCl3, AcOEt, 95% EtOH, and H_2O) as indicated in Table 5 and Fig. 2 indicated that AcOEt exhibited the lowest value for DPPH scavenging (IC_{50} = 18.6 ± 0.97 µg/mL), which differed slightly from the value for 95% EtOH extract (IC_{50} = 30.4 ± 1.86 µg/mL) compared with ascorbic acid (IC_{50} = 10.6 ± 0.8 µg/mL), while H_2O, CHCl3, and hexane extracts showed moderate to weak activities. However, the antioxidant potential possessed by plant extracts was most probably due to the presence of polyphenols, which exerted a reducing effect on DPPH free radicals.

Flavonoids were identified as the principal ingredients in the sample using the UHPLC-QTOF-MS/MS technology, with quercetin, kaempferol, and apigenin being the most prevalent [33]. Flavonoids are among the most numerous natural components found in diverse plants and have a wide variety of biological actions, including cytotoxic, antibacterial, and antioxidant effects [34]. Numerous studies have suggested that flavonoids' principal antibacterial actions involve the inhibition of nucleic acid production, the decrease of cell attachment, and the suppression of biofilm development [35, 36]. Table 2 shows that *Z. capitata* L. includes a variety of phenolic compounds, including luteolin, isorhamnetin, chlorogenic acid, apigenin, and rutin, These compounds have excellent antibacterial activities against a variety of microorganisms, including those used in the current investigation [37, 38]. Caffeic acid and chlorogenic acid, for example, have been shown to have antiproliferative effects, This action is thought to be due to the presence of two or more hydroxyl (OH) groups on the phenyl structure, which confers polyphenolic characteristics [39]. Furthermore, several phenolic compounds in *Z. capitata* L. have been demonstrated to have antimicrobial properties, as quercetin, which has been found to be an effective antibacterial agent against *S. aureus* and *S. epidermidis* [40]. Also, vitexin, kaempferol, quercetin-3-*O*-glucoside-7-*O*-rhamnoside, and kaempferol-4'-methyl ether have also been identified as antibacterial compounds [41]. The antibacterial properties of *Z. capitata* L. may also be attributed to other substances. It has been suggested by Adamczak et al.[33], Stavri and Gibbons [42] that the plant's coumarin content may be a factor in its enhanced antibacterial effect. Some flavonoids in *Z. capitata* L. have positive bioactivities as well. Acacetin and its glycosides are flavonoid compounds that have anti-mutagenic, anti-inflammatory, anti-peroxidant, anti-plasmodial, and anticancer properties [43]. Baicalein-7-*O*-glucuronoside has the highest concentration of the chemical components, according to the findings of the UHPLC-QTOF-MS/MS study of the plant. It was found that baicalin and its derivatives exhibited anti-diabetic characteristics, according to the reference [44]. Baicalein 7-*O*-β-D-glucuronide (baicalin) and baicalein have anti-cancer, anti-inflammatory, anti-viral, anti-fungal, and antioxidant activities [45]. Similarly, alkaloids found in *Z. capitata* L. May contributed to its antibacterial properties, several studies have shown that alkaloids have considerable biological activity [43]. Harmaline, an indole alkaloid found in a range of Malvaceae medicinal plants, has been shown to have antibacterial action as well as various other biological properties such as antioxidant and anti-inflammatory activity [46]. Ziziphora species have a long history of usage in traditional folk medicine to treat a wide range of serious ailments in various countries. Essential oils, extracts, and volatiles from several Ziziphora species exhibit cytotoxic, antibacterial, antioxidant, antifungal, and immune stimulant effects [10]. Several studies have shown that Ziziphora plants have antibacterial and antifungal properties against a wide range of microorganisms [47].

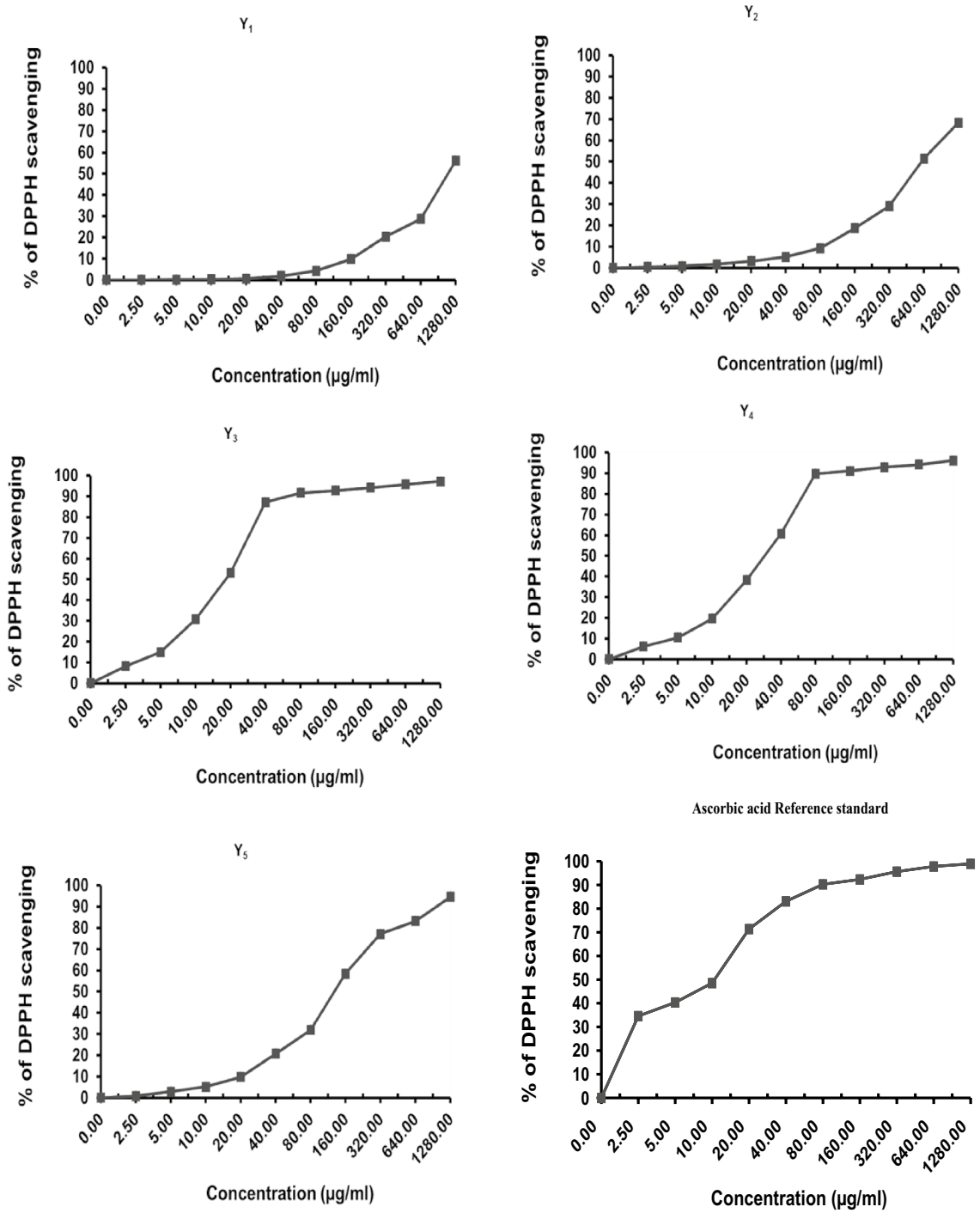


Fig. 2 DPPH results for successive extracts of *Z. capitata* (hexane Y_1, $CHCl_3$ Y_2, AcOEt Y_3, 95% EtOH Y_4, and H_2O Y_5)

3.5 Molecular docking simulation

In this work, the docking simulation of the top ten phytochemicals in *Z. capitata* L. MeOH extract (70%) in positive ionization mode using UPLC-QTOF-MS/MS technique was carried out inside the active site of *S. aureus* DNA gyrase (**PDB**: 2XCT) and dihydropteroate synthase (DHPS) from *S. pneumonia* (**PDB**: 2VEG) as bacterial targets as described previously [26–28]. The structure of the 3D of the DNA gyrase (**PDB**: 2XCT) and dihydropteroate synthase (DHPS) (**PDB**: 2VEG) bounded to the co-crystallized ligand were retrieved from the protein data bank (https://www.rcsb.org/) as described in Fig. 3.

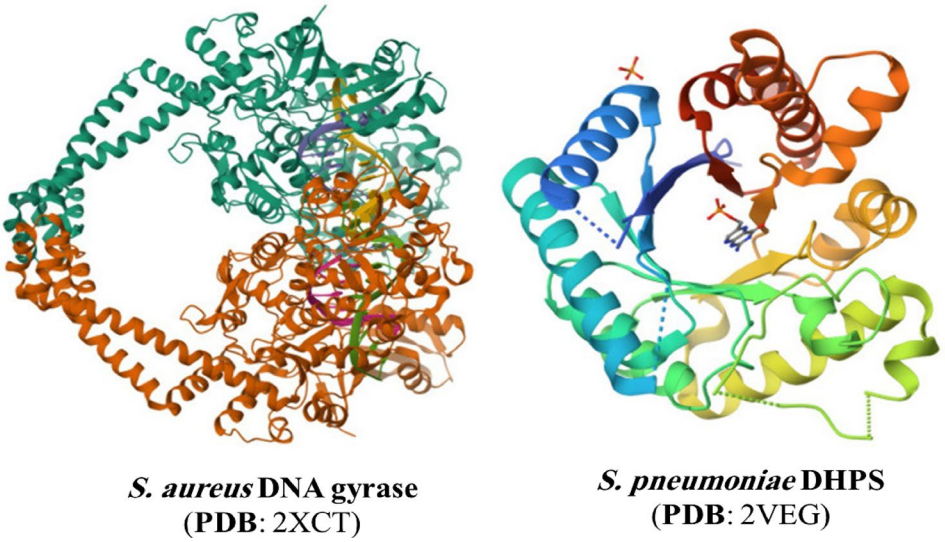


Fig. 3 3D structure of DNA gyrase (**PDB**: 2XCT) and dihydropteroate synthase (DHPS) (**PDB**: 2VEG) bounded to the co-crystallized ligand

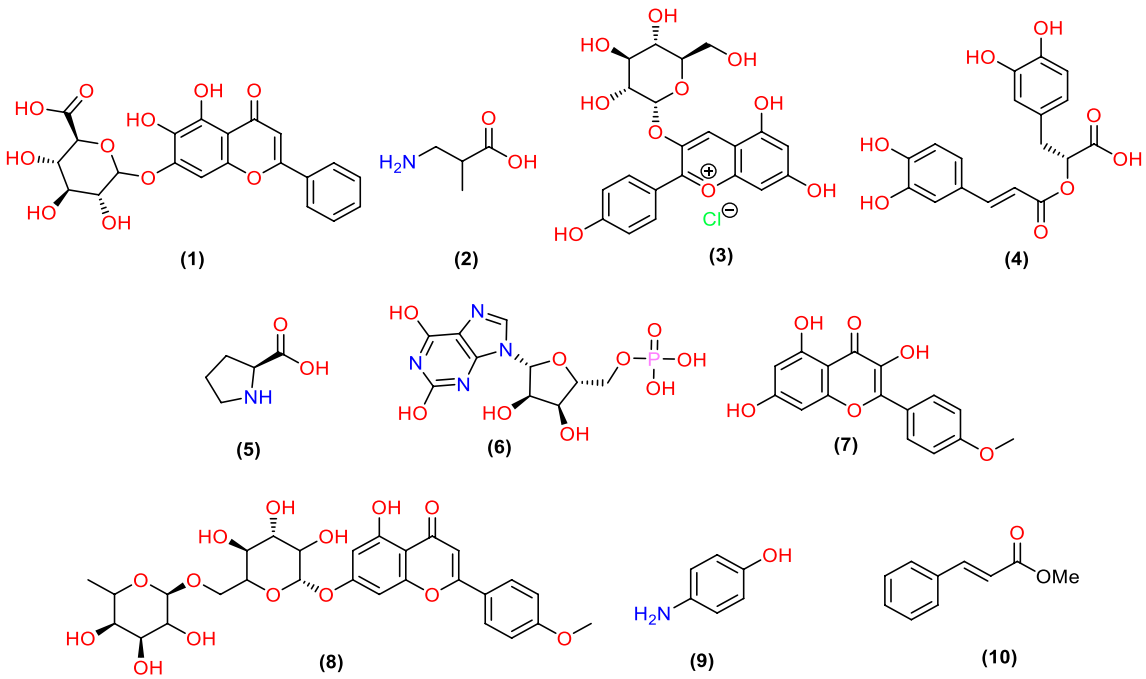


Fig. 4 The structure of the top ten concentrated compounds in *Z. capitata* L. MeOH extract (70%) in positive ionization mode using the UPLC-QTOF-MS/MS technique

The structures of the top ten concentrated compounds in *Z. capitata* L. MeOH extract (70%) in positive ionization mode using UPLC-QTOF-MS/MS technique are listed in Fig. 4 and represented by numbers from 1 to 10. The binding energy of each case for the tested phytochemicals represented by (S) kcal/mol and listed in Table 6 compared with co-crystallized ligand in each case with RMSD value and positive control drug for antibacterial activity. The docking simulation of the top ten phytochemicals was carried out inside the active site of DNA gyrase (**PDB**: 2XCT) and compared with the co-crystallized ligand (Ciprofloxacin) and positive control drug (Gentamycin). Firstly, the tested phytochemicals showed negative binding energies, indicating that these compounds could bind to the active sites to different degrees. In addition, the highest binding energy was observed by compound **1** (S = – 12.76 kcal/mol), followed by compound **8** (S = – 13.56 kcal/mol) and compound **3** with a value of – 14.77 kcal/mol. All these three phytochemicals showed binding energy higher than Ciprofloxacin (S = -12.60 kcal/mol with RMSD = 1.1179 Å) but lesser than that of gentamicin

Table 6 Docking simulation results represented by binding energy (S = kcal/mol) of top ten phytochemicals in *Z. capitata* L. methanolic extract using UPLC-QTOF-MS/MS technique

Phytochemical No.	DNA gyrase (PDB: 2XCT)	Dihydropteroate synthase DHPS (PDB: 2VEG)
1	− 12.76	− 12.47
2	− 7.15	− 10.57
3	− 14.77	− 14.56
4	− 11.89	− 14.17
5	− 8.46	− 9.36
6	− 9.86	− 12.78
7	− 10.02	− 12.01
8	− 13.56	− 13.57
9	− 7.24	− 9.08
10	− 7.89	− 9.62
Co-crystallized L/RMSD	− 12.60/1.1179	− 13.48/0.7813
Gentamycin	− 23.38	− 20.08

(S = − 23.38 kcal/mol). The other phytochemicals **2**, **4**, **5**, **6**, **7**, **9**, and **10** demonstrated moderate binding energies ranging from − 7.24 to − 11.89 kcal/mol.

For phytochemical **3**, the highest binding energy was S = − 14.77 kcal/mol through three hydrogen bonds. The pyranose ring formed two hydrogen bond backbone donors between Ala509 and the hydroxyl group at C-6 of the pyranose of pelargonidin-3-*O*-glucoside and Tyr1150 with the hydroxyl group at C-4 of the pyranose with a bond length of 1.7 and 2.1 Å and strength of 24 and 68%, respectively. In addition, Ser1028 interacted with the hydroxyl group of the phenyl moiety at C-2 of benzo[*b*]pyran with a distance of 2.5 Å and strength of 11%. Moreover, an arene-cation interaction occurred

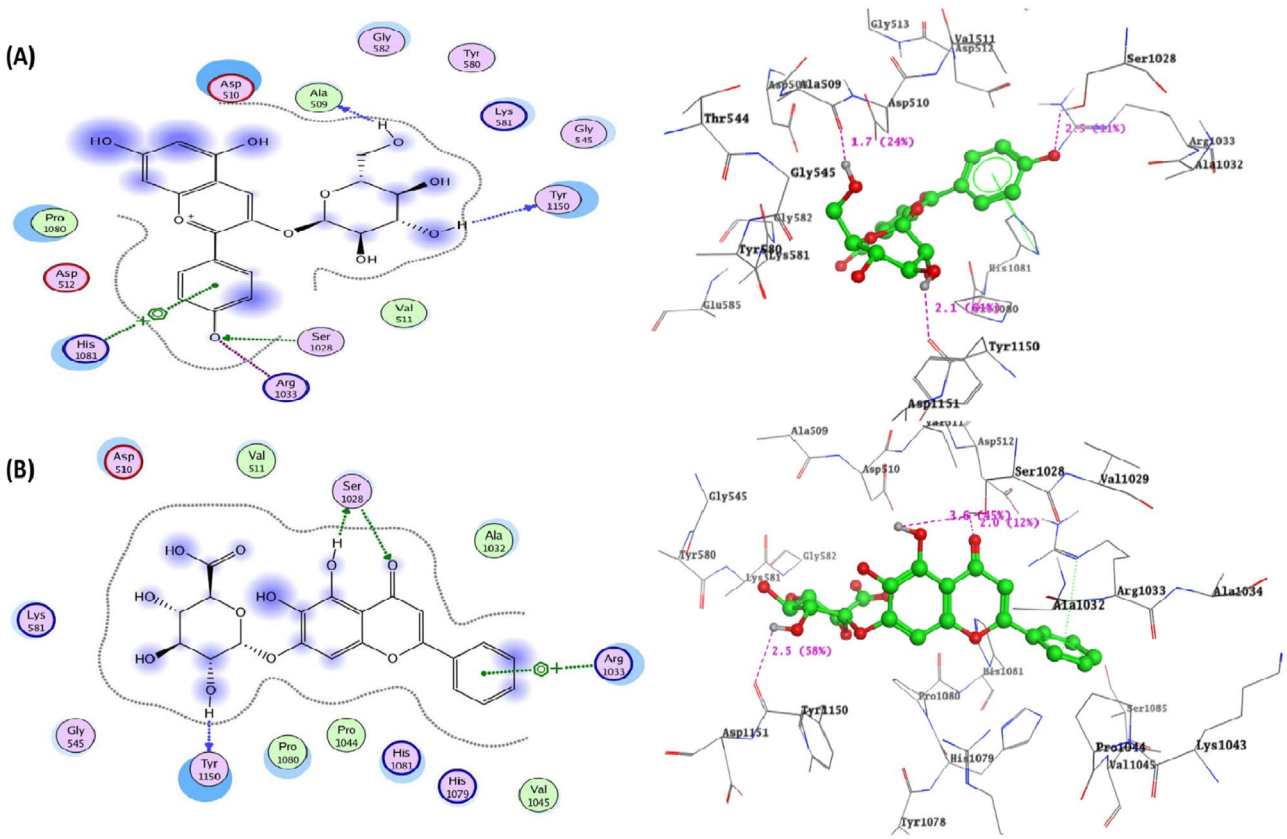


Fig. 5 2D and 3D of the best docking pose of (**A**) compound **3** and (**B**) compound **1** against the DNA gyrase (**PDB**: 2XCT)

between the key residue His1081 and the phenyl ring at C-2 of benzo[*b*]pyran pharmacophore of pelargonidin-3-*O*-glucoside, Fig. 5a. Simultaneously, baicalein-7-*O* glucuronide (1) displayed three hydrogen bonds with one arene-cation interaction with three residues, Ser1028, Tyr1150, and Arg1033. The Ser 1028 could form two hydrogen bonds from the side chain: one hydrogen bond donor with the oxygen atom of the carbonyl group of benzo[*b*]pyran with a bond length of 2.0 Å and strength of 12%, and the second hydrogen bond side chain acceptor with the oxygen atom of the hydroxyl group at C-5 of benzo[*b*]pyran moiety with a distance of 3.6 Å (45%). The third hydrogen bond formed between the hydroxyl groups at C-3 of the pyranose ring had a bond length of 2.5 Å and strength of 58%. The arene-cation interaction was demonstrated between Arg1033 and the phenyl ring at C-2 of baicalein-7-*O*-glucuronide, Fig. 5b.

Furthermore, compound **8** revealed five hydrogen bonds with two residues, Arg1033 and Ala1023. The key residue of DNA gyrase Arg1033 formed three hydrogen bond side chain acceptors with the oxygen of ether linkage at C7 of the benzo[b]pyran moiety and two bonds through the oxygen of pyranose ring with bond lengths of 2.2 Å (25%), 1.6 Å (56%), and 1.9 Å (29%), respectively Fig. 6a, b.

The antibacterial action may be associated with the three phytochemicals **1**, **3**, and **8** having greater binding energies than ciprofloxacin as a co-crystallized ligand. These three derivatives also showed higher binding energies than the other ten components. During the validation step of the docking method, the co-crystallized ligand demonstrated binding energy S = − 12.60 kcal/mol with RMSD = 1.1179 Å through two hydrogen bonds and one metal bond. The residue His1081 formed a hydrogen bond acceptor with the oxygen of carboxylate, with a bond length of 1.3 Å and strength of 37%. In comparison, a second hydrogen bond (backbone donor) was observed between Tyr580 and NH of the piperazine fragment, with a length of 1.5 Å and strength of 46%. Moreover, the key residue His1081 is bound by the oxygen of the carboxylate with an ionic bond Fig. 6. In addition, gentamycin, as a positive control for antimicrobial activity, exhibited binding energy S = − 23.38 kcal/mol and displayed many interactions inside the active site as three hydrogen-bond side chain donors with Asp510, two hydrogen-bond side chain donors with His1081, one side chain donor with Glu435, and one hydrogen-bond backbone acceptor with Val511. Moreover, gentamicin could form four ionic bonds, two ionic bonds (represented by the turquoise color) with Asp510, one with Glu435, and one with His1081, as well as many hydrophobic interactions with residues Asp508, Gly1082, Pro1080, Asp512, and Lys460, as represented in Fig. 7.

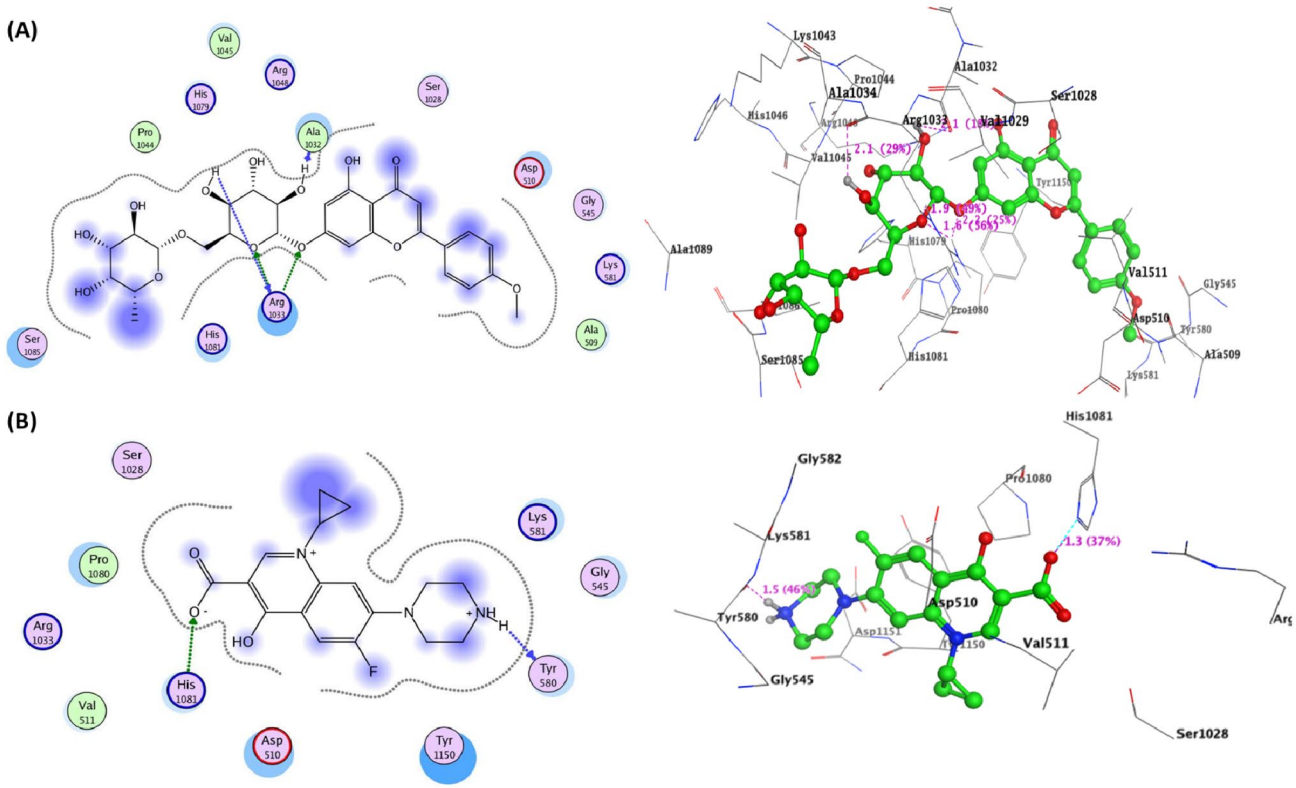


Fig. 6 2D and 3D of the best docking pose of (**A**) compound **8** and (**B**) co-crystallized ligand (Ciprofloxacin) against the DNA gyrase (**PDB**: 2XCT)

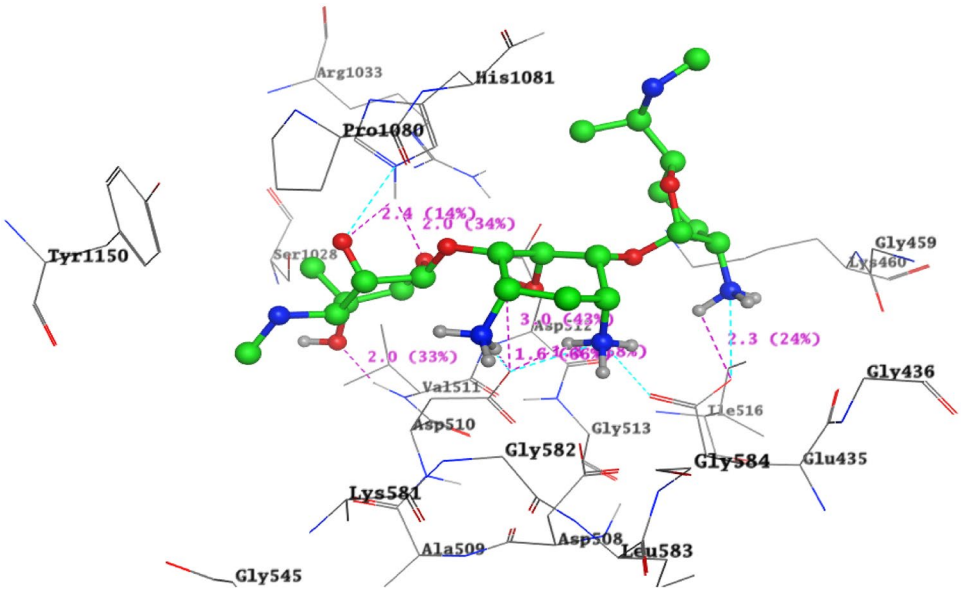


Fig. 7 3D of the best docking pose of Gentamycin against the DNA gyrase (**PDB**: 2XCT)

Furthermore, the affinity of the top 10 tested compounds was predicted against dihydropteroate synthase (DHPS) from *S. pneumoniae* (**PDB**: 2VEG), which catalyzes an essential step in the biosynthesis of folic acid in the folate cycle of bacteria. The results showed that the tested compounds exhibited binding energies ranging from − 9.08 to − 14.56 kcal/mol in contrast to 6-hydroxymethyl-7,8-dihydropterin monophosphate as a co-crystallized ligand (S = − 13.48 kcal/mol with RMSD = 0.7813 Å) and gentamicin (S = − 20.08 kcal/mol). Among the phytochemicals, compounds **3**, **4**, and **8** exhibited binding energies S = -14.56, -14.17, and -13.57 kcal/mol higher than the co-crystallized ligand S = − 13.48 kcal/mol, indicating that these derivatives may display significant binding energy as co-crystallized ligands at the atomic level. The phytochemical **3** revealed that the binding energy S = − 14.56 kcal/mol inhibited DHPS by interacting with Lys237 through a hydrogen bond acceptor from the side chain with a hydroxyl group at C-5 of benzo[*b*]pyran with a bond length of 2.1 Å and strength of 96%. Asp201 formed a hydrogen bond donor with a hydroxyl group at C-7 of benzo[*b*]pyran with a distance of 2.1 Å and a strength (score) of 10%. Finally, Ser235 is bound to the hydroxyl group at C-6 of the pyranose fragment through a hydrogen bond backbone donor with a bond length of 3.7 Å and strength of 13%. In addition, another interaction was observed with two rings of benzo[*b*]pyran with Arg282, known as arene-cation interactions, and many hydrophobic interactions were observed with the structure of the pelargonidin-3-*O*-glucoside with residues of Glu55, Asp91, Asn17, Ile112, Asn110, Met135, His284, and Arg236, as presented in Fig. 8a. On the other hand, compound **4** (rosmarinic acid) displayed one hydrogen bond donor between Asp91 and the hydroxyl group of the carboxylic group with a bond length of 2.2 Å and strength of 19, and two arene-cation interactions between Arg282 and Lys237 with two phenyl groups of rosmarinic acid. In addition, the orientation of phytochemicals in the pocket revealed many hydrophobic interactions with residue amino acids, such as Asn110, Gly233, Asp201, Met135, Arg238, Arg236, Asn17, Ile112, and Leu232 Fig. 8b. Furthermore, the third highest binding energy value was obtained by acacetin-7-*O*-rutinoside (**8**), which demonstrated a binding energy of S = − 13.57 kcal/mol through four hydrogen bond acceptors from the side chain with three residues, Asn17, Arg282, and 2*Lys237, with distances of 2.6 Å (29%), 2.2 Å (20%), 1.9 Å (47%), and 2.3 Å (62%), respectively. In addition, one hydrogen bond donor was found between Asp201 and the hydroxyl group at C5 of terminated pyranose with a bond length of 2.1 Å and strength of 23%, as shown in Fig. 9a. In addition, many hydrophobic interactions were observed between the ligand and Arg238, Arg236, His248, Ile112, Phe206, Met135, Asp91, and Gly233. To understand the effectiveness of the previous three phytochemicals based on the binding energy values and different types of interactions, these issues were compared with the validation process for the co-crystallized ligand inside the active site of dihydropteroate synthase (DHPS) from *S. pneumoniae* (PDB: 2VEG). The co-crystallized ligand showed a binding energy of S = − 13.48 kcal/mol with an RMSD = 0.7813 Å. These interactions were exhibited with different amino acid residues as follows: Asp201 (two hydrogen bond donors), Asn101 (one hydrogen bond acceptor and one hydrogen bond donor from sidechain), Arg288 (two hydrogen bonds side

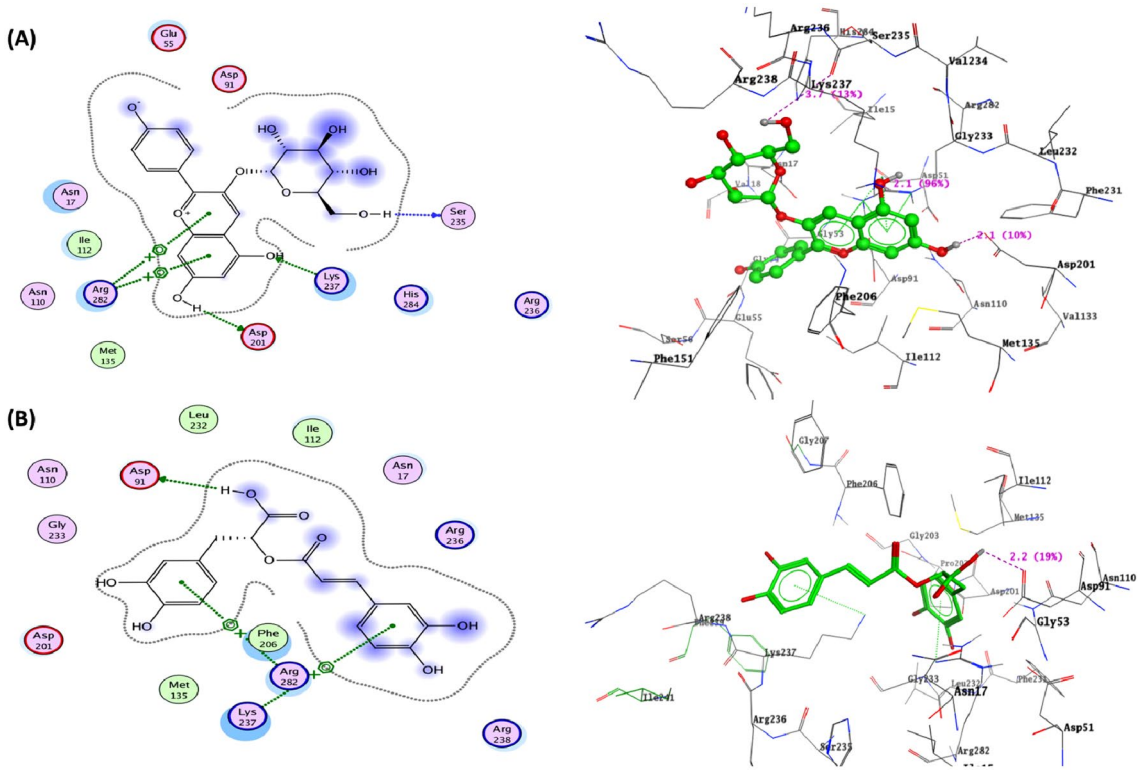


Fig. 8 2D and 3D of the best docking pose of (**A**) compound **3** and (**B**) compound **4** against the dihydropteroate synthase (DHPS) from *Streptococcus pneumoniae* (**PDB**: 2VEG)

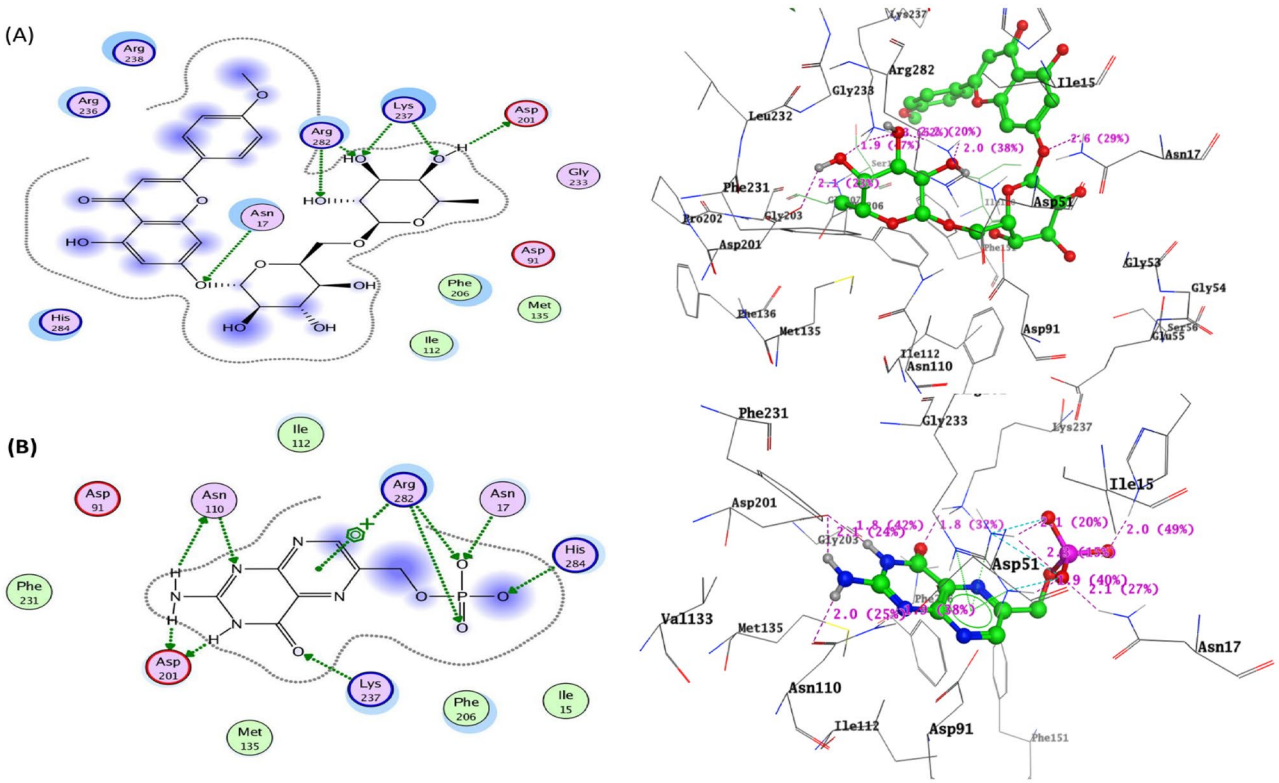


Fig. 9 2D and 3D of the best docking pose of (**A**) compound **8** and (**B**) co-crystallized ligand against dihydropteroate synthase (DHPS) from *Streptococcus pneumoniae* (PDB: 2VEG)

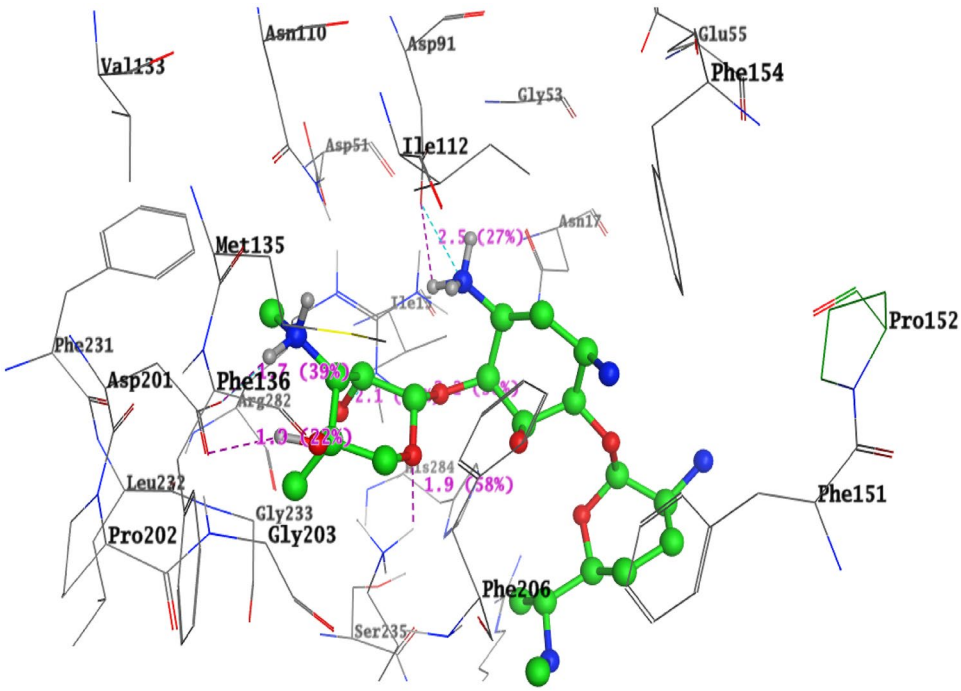


Fig. 10 3D of the best docking pose of Gentamycin against the dihydropteroate synthase (DHPS) from *Streptococcus pneumoniae* (**PDB**: 2VEG)

chain acceptor, one arene-cation interaction with the piperazine core, and three ionic bonds with oxygen of the phosphonate group), Asn17 (H-bond acceptor side chain), His284 (side chain acceptor H-bond), and Lys237 (H-bond acceptor) Fig. 9b. Moreover, gentamicin showed three hydrogen bond donors with 2*Asn201 and Asp91 and three hydrogen bond acceptors with 2*Arg282 and Lys237, as well as three ionic bond interactions with Asn201, Arg282, and Asp91, as shown in Fig. 10. All these interactions fitted the gentamicin well inside the active DHPS and therefore exhibited good antibacterial activity.

4 Conclusion

Throughout this investigation, UPLC-QTOF-MS/MS technology was employed to determine the presence of 78 bioactive constituents from total extract 70% EtOH of *Z. capitata* L. aerial parts. In vitro, the extracts also showed antibacterial efficacy against some Gram-negative and Gram-positive bacterial strains. For antioxidant activities, EtOH extract exhibited the lowest value for DPPH scavenging ($IC_{50} = 18.6 \pm 0.97$ µg/mL) compared with ascorbic acid ($IC_{50} = 10.6 \pm 0.8$ µg/mL). Docking simulation results of the top ten phytochemical compounds revealed that the antibacterial activity of the component in the positive mode may be attributed to DNA gyrase and/or dihydropteroate synthase as bacterial targets, which appear by blocking and inhibiting the active site of the pocket with different types of interactions. The antimicrobial and antioxidant activities of *Z. capitata* L. are likely due to the presence of active compounds such as phenolic compounds, flavonoids, coumarins, alkaloids, and anthocyanins, which have demonstrated good biological activities, particularly antibacterial and antioxidant activities. According to these findings, *Z. capitata* L. may be a viable natural product source. Finally, the molecular docking simulation predicted the possible binding mode and expected types of interactions inside the active site of the pocket.

Author contributions YMY collected the plant under study and wrote the main manuscript text, AR, MAZ, FAA, prepared all figures and contributed to the extraction process, GAME and AR wrote the molecular docking, and all authors reviewed the manuscript.

Funding There are no funding sources.

Data availability The data that support the findings of this study are available from the corresponding author upon reasonable request.

Declarations

Ethics approval and consent to participate Not applicable.

Consent for publication The authors agreed and gave their permission for the manuscript to be published.

Competing interests On behalf of all authors, the corresponding author states that there is no conflict of interest.

Open Access This article is licensed under a Creative Commons Attribution 4.0 International License, which permits use, sharing, adaptation, distribution and reproduction in any medium or format, as long as you give appropriate credit to the original author(s) and the source, provide a link to the Creative Commons licence, and indicate if changes were made. The images or other third party material in this article are included in the article's Creative Commons licence, unless indicated otherwise in a credit line to the material. If material is not included in the article's Creative Commons licence and your intended use is not permitted by statutory regulation or exceeds the permitted use, you will need to obtain permission directly from the copyright holder. To view a copy of this licence, visit http://creativecommons.org/licenses/by/4.0/.

References

1. Anand U, Jacobo-Herrera N, Altemimi A, Lakhssassi N. A comprehensive review on medicinal plants as antimicrobial therapeutics: potential avenues of biocompatible drug discovery. Metabolites. 2019;9(11):258. https://doi.org/10.3390/metabo9110258.
2. Vaou N, Stavropoulou E, Voidarou C, Tsigalou C, Bezirtzoglou E. Towards advances in medicinal plant antimicrobial activity: a review study on challenges and future perspectives. Microorganisms. 2021;9(10):2041. https://doi.org/10.3390/microorganisms9102041.
3. Alomar HA, Fathallah N, Abdel-Aziz MM, Ibrahim TA, Elkady WM. Gc-ms profiling, anti-helicobacter pylori, and anti-inflammatory activities of three apiaceous fruits' essential oils. Plants. 2022;11(19):2617. https://doi.org/10.3390/plants11192617.
4. Youssif MY, Ragab A, Abozeed MEA, Kobisi AA, Elhagali GA. Amino Acid Profile, in vitro Cytotoxic Activity of Herniaria hemistemon J. Gay Extract and Isolated Chemical Constituents with Reference to Molecular Docking Simulation. Chem. Africa. 2024. https://doi.org/10.1007/s42250-024-00997-0.
5. Elhagali GA, Abozeed AE, Youssif YM, Gay J. Investigation of bioactive constituents and biological activities of different fractions from Herniaria hemistemon J. Gay. Al-Azhar Bull Sci. 2019;30(1):67–80. https://doi.org/10.21608/absb.2019.67894.
6. Thabet HK, Ragab A, Imran M, Helal MH, Alaqel SI, Alshehri A, Ammar YA. Discovery of new anti-diabetic potential agents based on paracetamol incorporating sulfa-drugs: Design, synthesis, α-amylase and α-glucosidase inhibitors with docking simulation. Eur J Med Chem. 2024;275:116589. https://doi.org/10.1016/j.ejmech.2024.116589.
7. Salah EM, Issa MY, Mohamed TA, Hegazy MEF, Tadros SH, Fathallah N. Chemical composition and antifungal activity of Teucrium Leucocladum Boiss. essential oils growing in Egypt using two different techniques. Fut J Pharm Sci. 2024;10(1):51. https://doi.org/10.1186/s43094-024-00621-5.
8. Moghadam HD, Sani AM, Sangatash MM. Antifungal activity of essential oil of Ziziphora clinopodioides and the inhibition of aflatoxin B1 production in maize grain. Toxicol Ind Health. 2016;32(3):493–9. https://doi.org/10.1177/0748233713503.
9. Mohammadhosseini M. The ethnobotanical, phytochemical and pharmacological properties and medicinal applications of essential oils and extracts of different Ziziphora species. Ind Crops Prod. 2017;105:164–92. https://doi.org/10.1016/j.indcrop.2017.05.009.
10. Mohammadhosseini M, Akbarzadeh A, Hashemi-moghaddam H, Shahnama M, Fahimi B, Azami S. Gas chromatographic-mass spectrometric analysis of volatiles obtained by HS-SPME-GC-MS technique from aerial parts of *Ziziphora Capitata* L., and evaluation for biological activity. Orient J Chem. 2016;32(3):1439. https://doi.org/10.13005/ojc/320318.
11. Youssif YM, Elhagali GA, Zahran MA, Ahmed FA, Ragab A. Utilising UPLC-QTOF-MS/MS to determine the phytochemical profile and in vitro cytotoxic potential of *Ziziphora capitata* L. with molecular docking simulation. Nat Prod Res. 2024. https://doi.org/10.1080/14786419.2024.2335666.
12. Esmaeili A, Anaraki MT, Rustaiyan A, et al. Chemical composition and in vitro antibacterial activities of the oil of Ziziphora clinopodioides and Z. capitata subsp. capitata from Iran. Chem Nat Compd. 2008;44(3):387–9. https://doi.org/10.1007/s10600-008-9073-4.
13. Ibrahim SA, Ragab A, El-Ghamry HA. Coordination compounds of pyrazolone-based ligand: design, characterization, biological evaluation, antitumor efficiency, and DNA binding evaluation supported by in silico studies. Appl Organomet Chem. 2022;36:1–17. https://doi.org/10.1002/aoc.6508.
14. Rizk HF, El-Borai MA, Ragab A, Ibrahim SA. Design, synthesis, biological evaluation and molecular docking study based on novel fused pyrazolothiazole scafold. J Iran Chem Soc. 2020;17:2493–2505. https://doi.org/10.1007/s13738-020-01944-9.
15. Boulos L. Flora of Egypt, vol. 1. Cairo: Cairo Al Hadara Publ; 1999. p. 417.
16. Holmgren PK, Holmgren NH, Barnet LC. Index herbariorum of the world. Published online 1990.
17. Mohammed HA, Khan RA, Abdel-Hafez AA, et al. Phytochemical profiling, in vitro and in silico anti-microbial and anti-cancer activity evaluations and Staph GyraseB and h-TOP-IIβ receptor-docking studies of major constituents of Zygophyllum coccineum L. Aqueous-EtOH extract and its subsequent fractions: An approach to validate traditional phytomedicinal knowledge. Molecules. 2021;26(3):577. https://doi.org/10.3390/molecules26030577.
18. Balbaa SI. Chemistry of crude drugs. Cairo: Lab Manual Fac Pharmacy, Cairo Univ; 1986. p. 195.
19. Adegoke AA, Iberi PA, Akinpelu DA, Aiyegoro OA, Mboto CI. Studies on phytochemical screening and antimicrobial potentials of Phyllanthus amarus against multiple antibiotic resistant bacteria. Int J Appl Res Nat Prod. 2010;3(3):6–12.
20. Ellis BE. Natural products from plant tissue culture. Nat Prod Rep. 1988;5(6):581–612.
21. Ibrahim HS, Eldehna WM, Abdel-Aziz HA, Elaasser MM, Abdel-Aziz MM. Improvement of antibacterial activity of some sulfa drugs through linkage to certain phthalazin-1 (2H)-one scaffolds. Eur J Med Chem. 2014;85:480–6. https://doi.org/10.1016/j.ejmech.2014.08.016.

22. Yen GC, Der DuhP. Scavenging effect of EtOH extracts of peanut hulls on free-radical and active-oxygen species. J Agric Food Chem. 1994;42(3):629–32. https://doi.org/10.1021/jf00039a005.
23. Ayman R, Radwan AM, Elmetwally AM, Ammar YA, Ragab A. Discovery of novel pyrazole and pyrazolo[1,5-a]pyrimidine derivatives as cyclooxygenase inhibitors (COX-1 and COX-2) using molecular modeling simulation. Arch Pharm. 2023;356(2): e2200395. https://doi.org/10.1002/ardp.202200395.
24. Khattab ESAEH, Ragab A, Abol-Ftouh MA, Elhenawy AA. Therapeutic strategies for Covid-19 based on molecular docking and dynamic studies to the ACE-2 receptors, Furin, and viral spike proteins. J Biomol Struct Dyn. 2022;40(23):1–19. https://doi.org/10.1080/07391102.2021.1989036.
25. Eldeeb M, Sanad EF, Ragab A, et al. Anticancer effects with molecular docking confirmation of newly synthesized isatin sulfonamide molecular hybrid derivatives against hepatic cancer cell lines. Biomedicines. 2022;10(3):722. https://doi.org/10.3390/biomedicines10030722.
26. Basseem M, Emam AA, Kamal FH, Gamal AM, Abo Faraha SA. Photocatalytic activity of co-doped NPs based on ZnO as a new class of anti-microbial agents: synthesis, characterization, kinetics, isotherm, and in silico molecular docking simulation. Appl Organomet Chem. 2023;37(10):1–23. https://doi.org/10.1002/aoc.7238.
27. Saadon KE, Taha NMH, Mahmoud NA, Elhagali GAM, Ragab A. Synthesis, characterization, and in vitro antibacterial activity of some new pyridinone and pyrazole derivatives with some in silico ADME and molecular modeling study. J Iran Chem Soc. 2022;19(9):3899–917. https://doi.org/10.1007/s13738-022-02575-y.
28. Fayed EA, Mohsen M, El-Gilil SMA, Aboul-Magd DS, Ragab A. Novel cyclohepta[b]thiophene derivative incorporating pyrimidine, pyridine, and chromene moiety as potential antimicrobial agents targeting DNA gyrase. J Mol Struct. 2022;1262: 133028. https://doi.org/10.1016/j.molstruc.2022.133028.
29. Rizk HF, El-Borai MA, Ragab A, Ibrahim SA, Sadek ME. A novel of Azo-Thiazole moiety alternative for benzidine-based pigments: design, synthesis, characterization, biological evaluation, and molecular docking study. Polycycl Aromat Compd. 2023;43(1):500–22. https://doi.org/10.1080/10406638.2021.2015402.
30. Ragab A, Abusaif MS, Aboul-Magd DS, Wassel MMS, Elhagali GAM, Ammar YA. A new exploration toward adamantane derivatives as potential anti-MDR agents: design, synthesis, antimicrobial, and radiosterilization activity as potential topoisomerase IV and DNA gyrase inhibitors. Drug Dev Res. 2022;83:1305–30. https://doi.org/10.1002/ddr.21960.
31. Hassan AS, Morsy NM, Aboulthana WM, Ragab A. In vitro enzymatic evaluation of some pyrazolo[1,5-a]pyrimidine derivatives: design, synthesis, antioxidant, anti-diabetic, anti-Alzheimer, and anti-arthritic activities with molecular modeling simulation. Drug Dev Res. 2023;84(1):3–24. https://doi.org/10.1002/ddr.22008.
32. Javed M, Saleem A, Xaveria A, Akhtar MF. Daphnetin: a bioactive natural coumarin with diverse therapeutic potentials. Front Pharmacol. 2022;13: 993562. https://doi.org/10.3389/fphar.2022.993562.
33. Adamczak A, Ożarowski M, Karpiński TM. Antibacterial activity of some flavonoids and organic acids widely distributed in plants. J Clin Med. 2019;9(1):109. https://doi.org/10.3390/jcm9010109.
34. Imran M, Rauf A, Abu-Izneid T, et al. Luteolin, a flavonoid, as an anticancer agent: a review. Biomed Pharmacother. 2019;112: 108612. https://doi.org/10.1016/j.biopha.2019.108612.
35. Imran M, Salehi B, Sharifi-Rad J, et al. Kaempferol: a key emphasis to its anticancer potential. Molecules. 2019;24(12):2277. https://doi.org/10.3390/molecules24122277.
36. Gouda HM, Morsy AA, Youssef AK, Tolba IAEM, Hassan GOO. Phytochemical profile and antimicrobial assessment of Abutilon fruticosum Guill & Perr growing in Gebel Elba, Egypt. Egypt J Chem. 2022;65(132):1299–305.
37. Fu L, Lu W, Zhou X. Phenolic compounds and in vitro antibacterial and antioxidant activities of three tropic fruits: persimmon, guava, and sweetsop. Biomed Res Int. 2016. https://doi.org/10.1155/2016/4287461.
38. Wink M, Tomczyk M, Jakimiuk K, Wink M, Tomczyk M. Flavonoids of the Caryophyllaceae. Phytochem Rev. 2022;21(1):179–218. https://doi.org/10.1007/s11101-021-09755-3.
39. Yagasaki K, Miura Y, Okauchi R, Furuse T. Inhibitory effects of chlorogenic acid and its related compounds on the invasion of hepatoma cells in culture. Cytotechnology. 2000;33:229–35. https://doi.org/10.1023/A:1008141918852.
40. Liu R, Zhang H, Yuan M, et al. Synthesis and biological evaluation of apigenin derivatives as antibacterial and antiproliferative agents. Molecules. 2013;18(9):11496–511. https://doi.org/10.3390/molecules180911496.
41. HM R, NM N, LM AS. <The> lipid and flavonoidal constituents of Herniaria nemistemon J. gay and their biological activity. Published online 2006.
42. Stavri M, Gibbons S. The antimycobacterial constituents of dill (Anethum graveolens). Phyther Res an Int J devoted to Pharmacol Toxicol Eval Nat Prod Deriv. 2005;19(11):938–41. https://doi.org/10.1002/ptr.1758.
43. Li SP, Wang YW, Qi SL, et al. Analogous β-carboline alkaloids harmaline and harmine ameliorate scopolamine-induced cognition dysfunction by attenuating acetylcholinesterase activity, oxidative stress, and inflammation in mice. Front Pharmacol. 2018;9:346. https://doi.org/10.3389/fphar.2018.00346.
44. Froldi G, Djeujo FM, Bulf N, Caparelli E, Ragazzi E. Comparative evaluation of the antiglycation and anti-α-glucosidase activities of baicalein, baicalin (baicalein 7-O-glucuronide) and the antidiabetic drug metformin. Pharmaceutics. 2022;14(10):2141. https://doi.org/10.3390/pharmaceutics14102141.
45. Muderrisoglu C, Yesil-Celiktas O. High-yield biocatalysis of baicalein 7-O-β-d-glucuronide to baicalein using soluble helix pomatia-derived β-glucuronidase in a chemically defined acidic medium. Catal Letters. 2019;149:1701–9. https://doi.org/10.1007/s10562-019-02745-3.
46. Khan FA, Maalik A, Iqbal Z, Malik I. Recent pharmacological developments in β-carboline alkaloid "harmaline." Eur J Pharmacol. 2013;721(1–3):391–4. https://doi.org/10.1016/j.ejphar.2013.05.003.
47. Belmehdi O, Bouyahya A, Jekő J, et al. Chemical analysis, antibacterial, and antioxidant activities of flavonoid-rich extracts from four Moroccan propolis. J Food Process Preserv. 2021;45(10): e15816. https://doi.org/10.1111/jfpp.15816.

Publisher's Note Springer Nature remains neutral with regard to jurisdictional claims in published maps and institutional affiliations.